

# One-Dimensional Charring Rate Analysis from Malaysian Tropical Hardwoods: An Instrumental Measurement Approach

Hafizah Muhamad Azlan<sup>1,3</sup>, Zakiah Ahmad<sup>1\*</sup>, Norshariza Mohamad Bhkari<sup>2</sup> and Lannie Francis<sup>1,4</sup>

<sup>1</sup>Faculty of Civil Engineering, Universiti Teknologi MARA, 40450 Shah Alam, Selangor, Malaysia

<sup>2</sup>Institute for Infrastructure Engineering and Sustainable Management (IIISM), Universiti Teknologi MARA, 40450 Shah Alam, Selangor, Malaysia

<sup>3</sup>Civil Engineering Studies, Universiti Teknologi MARA, Cawangan Pulau Pinang, Permatang Pauh Campus, 13500 Permatang Pauh, Malaysia

<sup>4</sup>Faculty of Civil Engineering, Universiti Teknologi MARA, Sarawak Branch, Kota Samarahan Campus, 94300 Kota Samarahan, Sarawak, Malaysia

## ARTICLE HISTORY

Received : 16 July 2025

Accepted : 15 September 2025

Online : 31 March 2026

## KEYWORDS

charring rate,  
solid timber,  
hardwoods,  
fire resistance,  
instrumental measurement

## ✉ \* CORRESPONDING AUTHOR

Prof. Dr. Zakiah Ahmad  
Faculty of Civil Engineering,  
Universiti Teknologi MARA,  
40450 Shah Alam, Selangor,  
Malaysia  
Email: [zakiah@uitm.edu.my](mailto:zakiah@uitm.edu.my)

## ABSTRACT

Timber is naturally combustible, which makes timber structures vulnerable to fire. Hence, maintaining a balance between structural strength and fire resistance is crucial to ensure safety and durability. When exposed to high temperatures, timber undergoes thermochemical decomposition through pyrolysis, ignition, and char formation, altering its chemical composition and physical structure. The formation of a charred outer layer serves as an insulator, reducing heat penetration and protecting the core. This process makes the charring rate a critical parameter in fire-resistant design, influencing the structural performance and safety of timber under fire exposure. Therefore, this study examines the relationship between char depth and charring rate in five Malaysian tropical hardwood species (KerANJI, Resak, White Meranti, Kedondong, and Jelutong), with densities ranging from 450 kg/m<sup>3</sup> to over 1000 kg/m<sup>3</sup>. The timber samples were tested under standard fire exposure ISO 834 (equivalent to BS 476: Part 20), using a large furnace under one-dimensional charring conditions for a duration of 60 minutes, during which internal temperatures were continuously recorded via embedded thermocouples. The experimental data revealed significant interspecies variation in charring rates, with denser species such as KerANJI exhibiting slower char development than lower-density specimens like Jelutong. Charring rates were benchmarked against the Eurocode 5 (EC5)–recommended value of 0.5 mm/min, with most tested species performing favorably under the specified conditions. One-way ANOVA indicated statistically significant differences between species ( $p < 0.05$ ), supported by coefficient of variations (COV) values that demonstrated the reliability and repeatability of the observed trends. These findings contribute to critical baseline data for structural fire design in tropical regions, thereby improving the accuracy of charring rate estimation for local timber species. The results support the development of more tailored, performance-based fire safety strategies aligned with international standards.

© 2026 UMK Publisher. All rights reserved.

## 1. INTRODUCTION

Timber has long served as a construction material and remains relevant today due to its natural availability, sustainability, and structural performance. However, concerns about its fire resistance often lead to hesitation in its use for structural applications. As a combustible material, timber must be capable of sustaining design loads even under fire exposure. A critical factor in evaluating its fire performance is the charring rate, which measures the rate at which wood converts to char under high temperatures. This transformation affects the structural stability of timber during fire events. Timber combustion involves multiple stages, beginning with heating, followed by pyrolysis, which releases volatile gases and forms a protective char layer.

Timber combustion involves multiple stages, including heating, pyrolysis, and char formation, during which volatile gases are released and a protective char layer forms (Richter et al., 2021). The burning behavior is influenced by factors such as density, moisture content, and heat flux (Bartlett et al., 2019; Friquin, 2011). Flame heat feedback and char oxidation contribute significantly to the mass loss rate, with flame radiation accounting for up to 60% at peak mass loss (Morrisset et al., 2021). Char oxidation plays a crucial role in the energy balance, contributing 43-59% of the total heat release rate during steady-state burning (MacLeod et al., 2023). The interplay between chemistry and heat transfer is important at all stages of burning, unifying previous theories on wood pyrolysis (Richter et al., 2019). Understanding this

process is essential for assessing fire behavior, structural integrity, and ensuring safety in timber-based building design (Bartlett et al., 2019).

Wood decomposition during pyrolysis typically occurs in three stages: (1) removal of volatile components below 200 °C, (2) degradation of hemicellulose, cellulose, and lignin between 200–378 °C, and (3) formation of a residual char layer. The pyrolysis of wood is a superposition of the respective pyrolysis processes of these three components. Eurocode 5 (2004) specifies the location of the timber char line as the location of the 300 °C isotherms and provides a model for predicting the charring rate of timber. However, these data are based on European softwood and hardwood, whereas charring rate for tropical hardwoods might differ due to variations in density ranging from 450kg/m<sup>3</sup> to over 1000 kg/m<sup>3</sup>.

Charring rates influenced by material properties such as density, moisture content, and grain orientation, as well as external factors like thermal exposure and oxygen concentration (Friquin, 2011). Service loads can accelerate charring and increase charring depth, affecting the wood's fire behavior (Qin et al., 2021). Density has the greatest impact on charring rate, with higher density timber exhibiting lower charring rates (Liu & Fischer, 2024). However, tropical hardwoods possess unique structural and thermal properties that differentiate them from their temperate counterparts, necessitating localized research (Hugi et al., 2007). Studies have mentioned that there is no correlation between charring rate and density. Liu and Fischer (2024) and Osvaldova et al. (2023) highlighted significant variability in charring behavior among tropical species, emphasizing the need for empirical data to inform regional fire safety codes.

It is important to validate the current models in the Eurocode 5 (2004) using the experimental data. The aim is to gain a comprehensive understanding of the fire resistance of Malaysian hardwoods by applying the Eurocode 5 (2004) model. Moreover, fire design in Malaysian building practice is guided by provisions in the Uniform Building By-Laws 1984 (UBBL, 2024), which stipulate minimum fire resistance periods for structural members. Satisfying these requirements using local timber species requires accurate thermal and charring data under conditions replicating real-world fire exposure. At present, the Malaysia Standard, MS 544 : Part 9 (2001) (as in Table 1) has generalized the charring rate value for untreated timber by strength group rather than density, which differs from Eurocode 5 (2004).

To bridge this knowledge gap, it is necessary to assess the fire performance of Malaysian hardwoods through direct experimentation, thereby supporting the integration of

local species into performance-based fire safety design.

**Table 1.** Notional rate of charring for the calculation of residual section based on MS544:Part 9

| Species      | Charring Rate (mm/min) |
|--------------|------------------------|
| SG 1 to SG 3 | 0.5                    |
| SG 4 to SG 5 | 0.7                    |

*Note: Strength Group refers to MS544 : Part 2*

The charring rate values are compared with Eurocode 5 (2004) benchmarks to evaluate compliance and suitability for structural use. Statistical methods, including one-way ANOVA, are employed to assess interspecies variability, while temperature-time and charring depth curves provide insight into thermal degradation behavior. The findings serve as a scientific foundation for incorporating tropical hardwoods into fire-safe structural applications, particularly in regions with similar climatic and material contexts.

### 1.1. One-Dimensional Charring

The one-dimensional charring rate of wood is one of the fundamental parameters used to determine the fire resistance of wooden structures. Numerous studies have shown that the charring rate primarily depends on factors such as wood density, fire exposure duration, and thermal conditions. Experimental observations also demonstrate variability in charring rates depending on wood species and fire conditions. For instance, Douglas fir beams showed average horizontal and vertical charring rates of 0.98 mm/min and 1.08 mm/min, respectively, under prolonged exposure (Zhang et al., 2012). Similarly, spruce and pine exhibited charring rates between 0.67 and 1.50 mm/min, influenced by both heat flux and exposure duration (Martinka et al., 2018). A wide range of experimental methods and numerical simulations, such as finite element modelling, have been employed to assess charring progression and internal temperature distribution within timber structures.

While many of these studies highlight the effects of exposure time and density, it is also essential to consider the timber type and species tested. Different wood types, particularly tropical hardwoods, may exhibit unique fire resistance characteristics due to their varied anatomical structures, thermal properties, and combustion behaviour (Njankou et al., 2004). Therefore, this study investigates the one-dimensional charring rate of five selected Malaysian tropical hardwood species, using controlled furnace tests conducted in accordance with standard fire exposure protocols.

It is important to clarify that this study specifically focuses on solid tropical hardwoods and is not comparable

with studies examining laminated veneer lumber (LVL) made from tropical species (Bakri & Ahmad, 2025). Although both may use similar wood sources, their structural composition and fire behaviour differ significantly. For instance, LVL includes bonded layers with adhesives and has different thermal conductivity compared to natural solid wood. This distinction is recognised in the Eurocode 5 (2004), which provides separate design charring rates ( $\beta_0$ ) for each timber product type. According to Table 3.1 of the Eurocode 5 (2004), solid or glued laminated hardwood with a density of  $\geq 450 \text{ kg/m}^3$  is assigned  $\beta_0 = 0.50 \text{ mm/min}$ , whereas LVL, listed separately, has  $\beta_0 = 0.65 \text{ mm/min}$  for density  $\geq 480 \text{ kg/m}^3$ . This differentiation underscores the need to evaluate each material category independently.

As such, the findings of this study are not directly comparable with those related to LVL and provide novel data specific to solid tropical hardwoods. These results aim to support the refinement of fire design models, particularly for countries like Malaysia, where local species are underrepresented in current standards.

The theoretical foundation for one-dimensional charring rate is presented in the Eurocode 5 (2004), which defines the design charring rate ( $\beta_0$ ) under standard fire exposure conditions. The model assumes a wide or semi-infinite timber slab, unprotected and free from fissures, with fire exposure on one side (Figure 1). These conditions also apply to thin slabs or wide cross-sections situated away from edges and corners. The charring rate ( $\beta_0$ ) can be expressed as Equation 1.

$$\beta_0 = \frac{d}{t} \quad (1)$$

where,  $\beta_0$  = one-dimensional design charring rate under standard fire exposure,  $d$  = charring depth for one-dimensional charring,  $t$  = time of fire exposure.

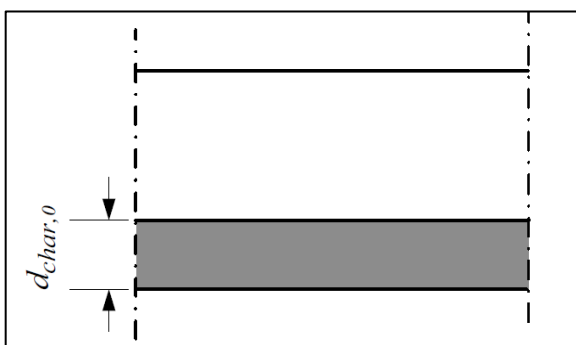


**Figure 1.** One-dimensional charring of wide cross-section with fire exposure on one side

## 2. MATERIALS AND METHODS

### 2.1. Specimens and Furnace Preparation

The wide range of densities represented by the timber species used in this study enables an assessment of fire resistance performance across multiple density categories. Five hardwood species—Keranji, Resak, White Meranti, Kedondong, and Jelutong—were chosen based on their availability in the local timber industry and potential for structural use. These species were grouped to represent the light, medium, and heavy hardwood categories in decreasing order of density, ranging from approximately  $590 \text{ kg/m}^3$  to  $960 \text{ kg/m}^3$ .

Each timber specimen was prepared to dimensions of  $100 \text{ mm} \times 100 \text{ mm} \times 1400 \text{ mm}$ , conforming to the size of the test frame used in the fire resistance furnace. All specimens were visually graded by a certified timber grader from the Malaysian Timber Industry Board (MTIB) in accordance with the grading requirements outlined in MS 1714, to ensure consistency in mechanical quality and structural integrity.

Each specimen was instrumented with six thermocouples (TC1–TC6) embedded at depths of 6, 12, 18, 24, 30, and 36 mm to monitor interior temperature profiles during fire exposure. Type K thermocouples, 4.8 mm in diameter and capable of withstanding temperatures up to  $1200 \text{ }^\circ\text{C}$ , were used in this study. These thermocouples were connected to a digital data logger to capture real-time temperature data throughout the heating process. Thermocouple lengths of 100, 200, and 300 mm were used, depending on their embedded depth. The thermocouple layout followed the protocol specified in EN 13381-7 (2019) for assessing temperature development within structural timber elements. The instrumentation layout is depicted in Figure 2.

Once instrumented, the specimens were installed horizontally within a custom-designed refractory furnace frame made of fire-resistant cement. The furnace frame was equipped with three horizontal slots to accommodate three specimens per fire test. All gaps between the specimens and the furnace wall were sealed using rock wool insulation blankets to minimize thermal leakage and ensure uniform heat exposure across the fire-facing surface. Figures 3 and 4 illustrate the furnace setup and the specimens with attached thermocouples.

Fire tests were conducted under one-sided exposure following the ISO 834 (1999) standard time-temperature curve. The gas-fired furnace had internal dimensions of  $1.5 \text{ m} \times 1.5 \text{ m} \times 1.5 \text{ m}$ . The furnace temperature was regulated and monitored remotely by trained personnel using three

calibrated plate thermometers, two on the left wall (top and bottom) and one on the right wall. The furnace control system was programmed to follow the ISO 834 (1999) standard time-temperature curve, defined by Equation (2):

$$T = 345 \log_{10}(8t + 1) + 20 \quad (2)$$

where, T is the furnace temperature (°C); t is the time (in min).

For each species, three specimens were prepared and were tested together in one frame. Samples were labeled A, B, and C, corresponding to their vertical position in the furnace frame (top to bottom), to account for possible thermal stratification. The fire within the furnace was assumed to spread uniformly across the exposed surface of the specimens.

In accordance with Clauses 213 and 214 of the UBBL (2024), which stipulate a minimum fire resistance requirement of 30 to 60 minutes for structural components, each specimen was subjected to 60 minutes of standard fire exposure. After the target exposure duration, heating was stopped, and the specimens were removed and quenched with water to prevent further pyrolysis beyond the controlled test period.

A minimum cooling period of 24 hours was allowed after each fire test, enabling the furnace to return to ambient conditions. This procedure ensured thermal stabilization and maintained the consistency and repeatability of the test environment for subsequent specimen exposures.

## 2.2. Assessment of Charring Rate

The charring rate for the one-dimensional specimens was determined in accordance with EN 13381-7 (2019). According to this standard,  $t_{300}$  denotes the time at which a thermocouple positioned on the surface or at a specified depth within an unprotected timber specimen reaches 300°C. Using the recorded times ( $t_{300,i,j}$ , in minutes), the charring rate ( $\beta_{i,j}$ ) was calculated between two consecutive depths (d), while the mean charring rate ( $\beta_j$ ) was determined for all measurement stations (j). The calculation of the charring rate is presented in Equation 3.

$$\beta_{i,j} = \frac{d_{i+1} - d_i}{t_{300,i+1} - t_{300,i}} \quad (3)$$

When no measurement was available for TC0 (the thermocouple positioned at the specimen surface), the start of charring was assumed to occur at  $t = 0$  min.

## 3. RESULT AND DISCUSSION

### 3.1 Temperature-Time Profile

The fire resistance performance of tropical hardwood species was monitored over a 60-minute period under standard ISO 834 (1999) fire exposure. Figure 5 presents the temperature-time curves for each timber specimen, obtained from thermocouples (TC1 to TC6) embedded at 6 mm intervals from the exposed surface, alongside the ISO 834 (1999) standard curve and the average furnace temperature curve. In all tests, temperatures showed a continuous upward trend, consistent with the programmed furnace profile, confirming the validity of the exposure regime.

In general, the temperatures recorded by thermocouples in all timber specimens displayed progressive increases with time. However, variations in temperature readings were observed across specimens, even at the same depths. This disparity is primarily attributed to inherent differences in thermal conductivity, density, moisture content, and structural anisotropy of the timber species, as well as potential surface cracking during combustion that may have influenced local heat transfer. Similar intra-species thermal variability under fire exposure have been reported by other researchers (Luptáková et al., 2019; Wen et al., 2015; Werther & Matthäus, 2020).

A key benchmark in fire analysis is the 300 °C isotherm, which is commonly accepted as the threshold for the onset of pyrolysis and char formation in lignocellulosic materials. The current findings indicate that for the majority of species, the 300 °C isotherm extended only up to TC3 (18 mm), with a few species reaching as far as TC4 (24 mm), while none reached TC6 (36 mm), suggesting that the charring front did not advance beyond this depth within the 60-minute exposure period. Accordingly, temperature readings from TC6 were excluded from the charring-depth analysis.

All curves followed a consistent pattern: temperature increases were steeper near the exposed surface (e.g., TC1 and TC2), while deeper thermocouples show delayed and moderated thermal responses. This behavior aligns with the expected heat transfer dynamics in wood, where conductivity is low and heat penetrated primarily by conduction. Notably, several specimens exhibit a distinct plateau or stagnation zone around 100 °C, particularly evident from TC2 to TC4, which corresponds to the evaporation of free and bound water within the timber matrix. Figure 6 shows water evaporation in some specimens during the fire test. The latent heat of vaporization significantly slows the temperature rise at this stage, consistent with earlier studies by and (Frangi & Fontana, 2003).

Moreover, the time required to reach 100 °C varied across species, reflecting differences in initial moisture content (MC). For instance, Kedondong and Resak, which had relatively higher MC values (see Table 2), exhibited delayed temperature rise in deeper thermocouples, supporting the thermal buffering role of water during the initial heating phase. Upon reaching and surpassing 150–200 °C, wood begins to thermally degrade, initiating depolymerization of hemicellulose and cellulose, and volatilization of organic compounds (Friquin, 2011).

At temperatures above 200 °C, lignin decomposition became dominant, contributing to the formation of char and release of gases such as CO, CO<sub>2</sub>, and CH<sub>4</sub> (Bartlett et al., 2019b). This progressive breakdown is visually represented in

the increasingly rapid temperature escalation seen in the outer thermocouples (e.g., TC1) after 20–30 minutes. The transformation from smooth to undulating profiles, especially at TC1 and TC2, indicated local instabilities in combustion and heat flux, possibly induced by surface cracking and flame flickering, phenomena commonly reported in solid timber fire testing.

In tropical hardwoods, where species-specific thermal inertia, moisture content, and structural characteristics interact to influence heat transport and char formation, the temperature–time profiles collectively demonstrate clear evidence of staged thermal reactions. The interpretation of charring behavior in the next sections is based on these thermal observations.

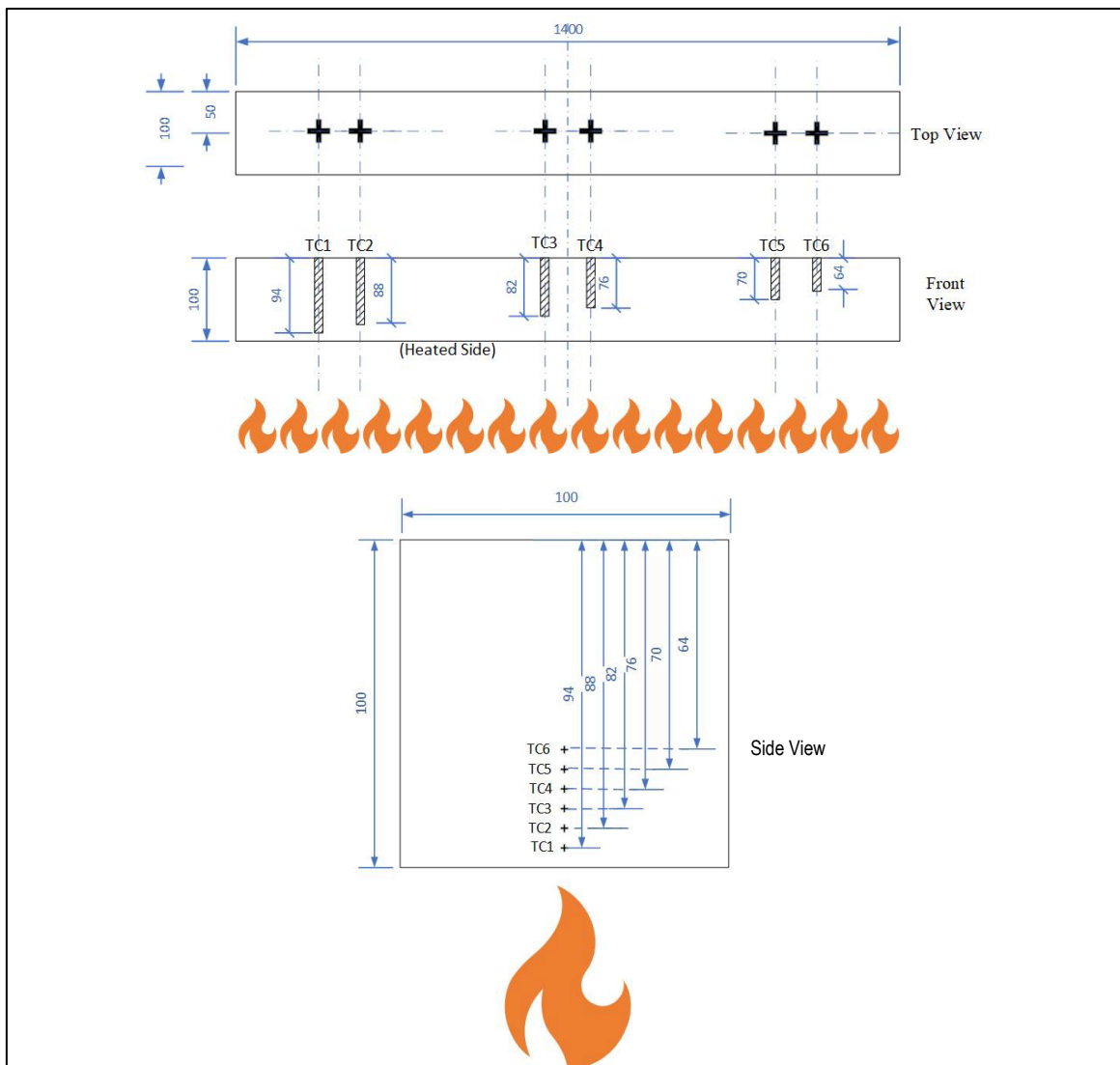


Figure 2. Thermocouple Layout for the Timber Specimens (all measurements in mm Units and not to scale)



Figure 3. Frame used to place the specimens in position, with gaps filled using rock wool for insulation.



Figure 4. Specimens have been installed and ready for fire test

### 3.2 Development of Char Depth of Solid Timber

As highlighted by several researchers (Cachim & Franssen, 2010; Frangi & König, 2011; Wang et al., 2025) timber loses significant strength and stiffness and becomes incapable of bearing load at the 300°C isotherm, as specified by Eurocode 5 (2004). Thus, charring depth in this study was determined at the depths where the thermocouples reached the 300°C isotherm. Figure 7 presents the charring depth as a function of exposure time for the five Malaysian tropical hardwood species tested.

All species consistently reached 300 °C at the 6 mm depth at all fire duration, except one Keranji specimen, which did not. This outlier was likely due to a defective thermocouple, an occurrence acceptable under standard testing protocols such as EN 13381-7 (2019). Notably, samples from Resak and White Meranti achieved the 300 °C isotherm at a depth of

30 mm after 60 minutes of exposure, indicating deeper heat penetration and potentially lower thermal resistance under prolonged heating.

One sample specimen from each species was chosen to compare the development of char depth over time to assess charring behavior. The time taken for each thermocouple to reach 300 °C at increasing depths was used to calculate char depth. As predicted, Jelutong and other lower-density species reached the critical isotherm faster, suggesting lower heat resistance and faster thermal diffusion. For example, it took 21.7 minutes for Jelutong to reach 300°C at a depth of 6 mm.

Interestingly, Resak, despite its medium-to-high density, showed comparable charring onset at the same depth within 21.9 minutes. This deviation from the expected trend may be attributed to compositional factors, particularly its

lignin and extractive contents, which can accelerate pyrolysis despite higher density.

The thermal behaviors of lignin-rich species is unique, especially in the 200–400 °C range, which is essential for their thermal softening and breakdown. Lignin normally starts to thermally decompose beyond 200 °C, with substantial mass loss and decomposition taking place between 250 and 450 °C. This range is characterized by the generation of various volatile compounds and the volatilization of primary lignin constituents. This supports the interpretation that charring onset is not solely governed by density but also by the wood's chemical constituents and moisture retention capacity.

Additionally, Figure 7 shows that after 60 minutes, most species reached 300°C up to a maximum depth of 24 mm, while Resak reached 30 mm. This demonstrates that the species was more vulnerable to structural deterioration over extended fire exposure because of its comparatively higher thermal diffusivity and potential decreased resistance to deep heat penetration. The time sequence for attaining the charring threshold followed the order Resak < Jelutong < Keranji < Kedondong < White Meranti. This order suggests that the initiation of charring is not strictly density dependent, but instead influenced by a combination of anatomical structure, moisture distribution, and the proportion of thermal-degradable polymers, particularly hemicelluloses and lignin. Hemicelluloses begin to thermally degrade at 200–260 °C, followed by the onset of lignin decomposition at 280–400 °C, which proceeds steadily up to 700 °C due to its complex and thermally stable aromatic structure (MacLeod et al., 2023; Richter et al., 2019). The broader decomposition range of lignin compared to cellulose and hemicelluloses implies that species with higher lignin content may undergo gradual but sustained charring across depth.

This behavior is further supported by thermal stagnation observed around 100–150 °C in earlier temperature–time graphs, corresponding to moisture evaporation. This process delays heat conduction initially but accelerates thermal degradation once the wood dries. Therefore, early onset of charring in Resak and Jelutong may be linked to their moderate to high moisture content, which, once evaporated, promotes rapid pyrolysis.

While density plays a central role in regulating charring behavior, these results affirm that thermal response is a multi-factorial process governed by species-specific physical and chemical properties. The interpretation of char

depth over time not only aids in understanding fire propagation mechanisms in solid timber but also provides foundational data for structural fire design based on time–temperature–depth relationships.

### 3.3 Quantification and Correlation of One-Dimensional Charring Rate with Density and Moisture Content

The charring rate of timber is a key performance indicator in fire resistance analysis, as it directly reflects the rate of material degradation under elevated temperature exposure. In this study, the charring rate values of the five hardwood species evaluated and interpreted. Statistical indicators such as standard deviation (SD) and COV were used to assess the variability and reliability of the observed measurements and are presented in Table 2.

The analysis revealed a generally inverse relationship between timber density and charring rate, consistent with the performance of denser species such as Keranji (959 kg/m<sup>3</sup>), which exhibited a relatively low mean charring rate of 0.22 mm/min. However, despite its slow degradation, Keranji showed a high COV at 51.6%, indicating substantial inconsistency likely influenced by internal grain orientation or non-uniform moisture distribution. In contrast, White Meranti (856 kg/m<sup>3</sup>), also a high-density species, recorded the lowest charring rate at 0.12 mm/min with a low COV of 6.8%, indicating a slow and stable charring process. This observation challenges the conventional assumption that lower-density timbers chars more quickly, underscoring the potential influence of anatomical structure and moisture dynamics over density alone.

A one-way ANOVA was conducted, confirming statistically significant differences in charring rate across species ( $F = 9.615$ ,  $p < 0.001$ ), suggesting these variations are not random but attributable to inherent anatomical and physical traits. Post-hoc tests ( $\alpha = 0.05$ ) further delineated species-specific groupings. Keranji and Jelutong, despite large differences in density, did not show statistically significant differences in charring rate, implying that factors such as grain configuration and moisture diffusion pathways may moderate the density-charring relationship. Similarly, Resak did not differ significantly from White Meranti or Kedondong, indicating that medium-density timbers may exhibit overlapping fire performance characteristics with lower-density species when accounting for moisture and structural variation.

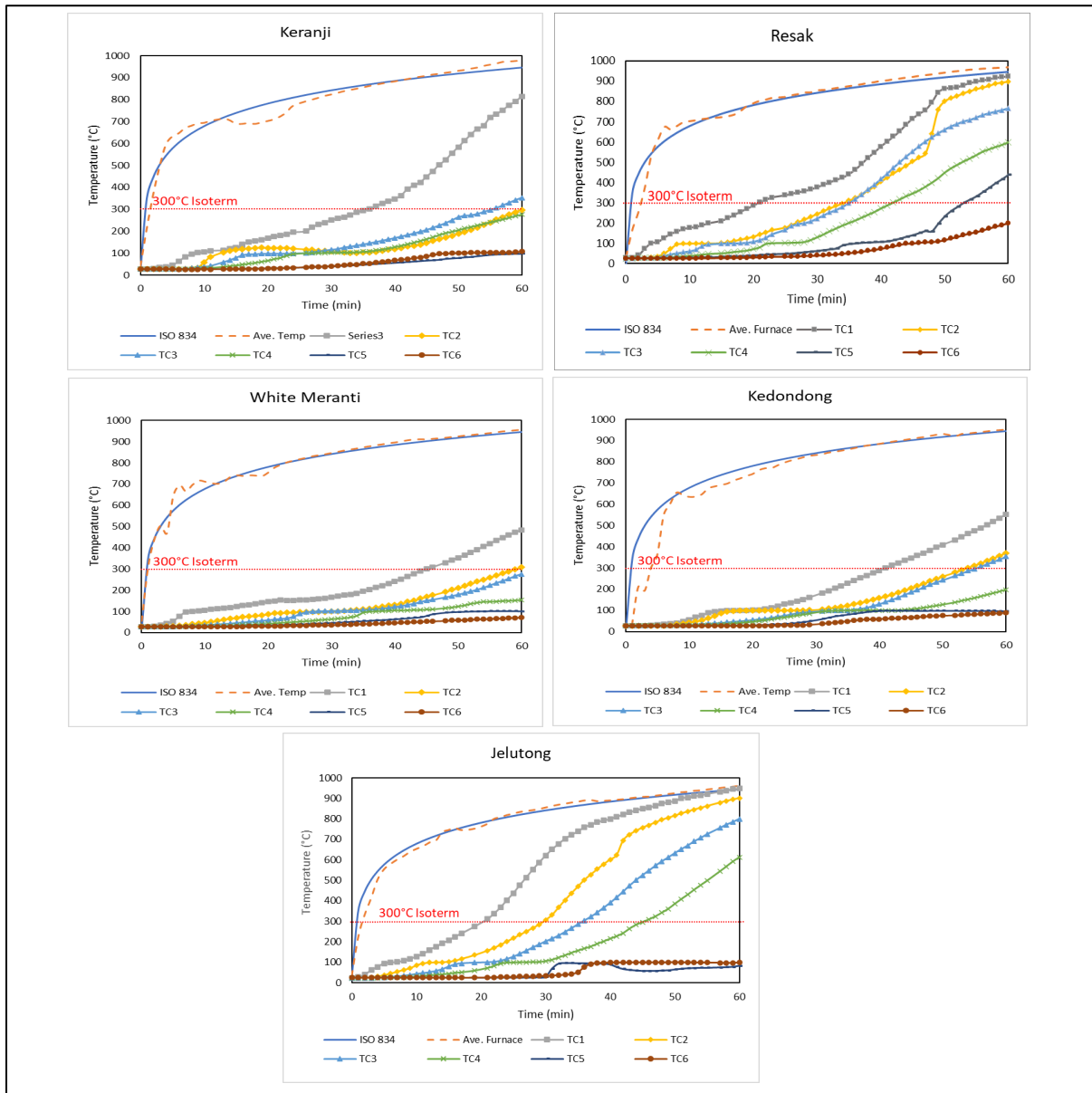


Figure 5. Typical Temperature -Time curve for all species

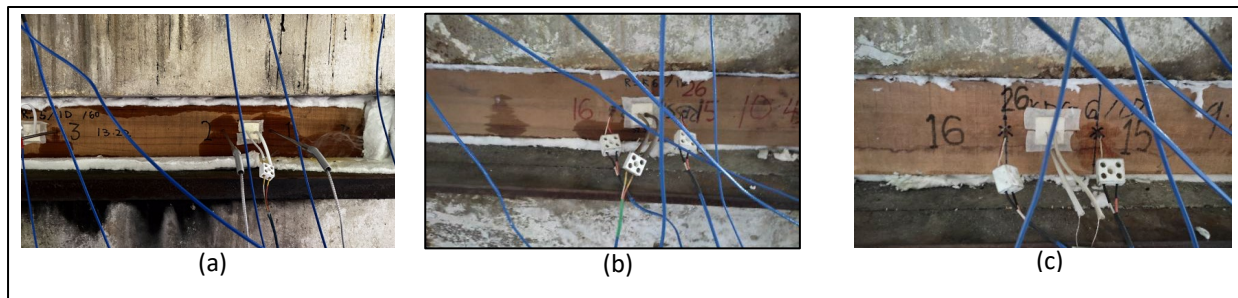


Figure 6. Water evaporation observed in (a) Keranji, (b) Resak and (c) Kedondong at the specimens surface

MC was also found to significantly affect thermal degradation. Jelutong, the least dense species ( $596 \text{ kg/m}^3$ ) with a moderate MC of 18.5%, displayed the highest charring rate of  $0.46 \text{ mm/min}$  and a COV of 29.3%. Moisture delays ignition but may lead to more intense pyrolysis once boiling occurs, especially in porous, low-density species (Friquin,

2010).

Kedondong, another low-density species, exhibited a moderate charring rate ( $0.17 \text{ mm/min}$ ) but high variability (COV = 48.1%), despite having a consistent MC (COV = 2.6%). This suggests that MC stability alone does not guarantee predictable charring performance, highlighting the

role of anatomical irregularities in influencing fire behavior. Furthermore, the performance of Resak (799 kg/m<sup>3</sup>) further illustrates the complexity of these interactions. This medium-density species showed a moderate charring rate of 0.40 mm/min with a COV of 28.5%, consistent with expectations for its density class. However, its relatively high MC variability (COV = 7.0%) likely contributed to fluctuations in char formation, reinforcing the notion that both density and MC jointly affect degradation behavior.

Collectively, these findings suggest that while density remains a useful predictor of charring rate, it must be interpreted alongside moisture content and anatomical factors. Charring behavior is not strictly linear or determined by any single variable but emerges from a complex interplay of density, moisture dynamics, and wood microstructure.

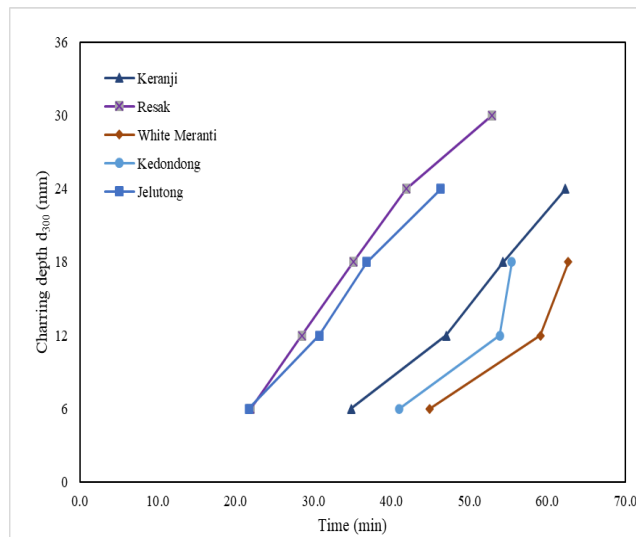


Figure 7. Char depth versus time for one-dimensional fire test

Table 2. Descriptive Analysis of Charring Rate for One-Dimensional Fire Exposure

| Species       | Type of Hardwood | Density                                 |                                  |             | Moisture Content     |                 |             | Charring Rate               |                      |             |
|---------------|------------------|-----------------------------------------|----------------------------------|-------------|----------------------|-----------------|-------------|-----------------------------|----------------------|-------------|
|               |                  | Mean ( $\bar{x}$ ) (kg/m <sup>3</sup> ) | Std Dev (s) (kg/m <sup>3</sup> ) | COV (v) (%) | Mean ( $\bar{x}$ ) % | Std Dev (s) (%) | COV (v) (%) | Mean ( $\bar{x}$ ) (mm/min) | Std Dev (s) (mm/min) | COV (v) (%) |
| Keranji       | Heavy            | 959                                     | 11.9                             | 1.2         | 17.2                 | 0.2             | 1.1         | 0.22 <sup>e</sup>           | 0.1                  | 51.6        |
| Resak         | Medium           | 799                                     | 40.5                             | 5.1         | 20.7                 | 1.5             | 7           | 0.40 <sup>c,d</sup>         | 0.1                  | 28.5        |
| White Meranti | Light            | 856                                     | 21                               | 2.5         | 19.2                 | 0.2             | 1.1         | 0.12 <sup>b</sup>           | 0                    | 6.8         |
| Kedondong     | Light            | 698                                     | 5.9                              | 0.8         | 22.1                 | 0.6             | 2.6         | 0.17 <sup>b</sup>           | 0.1                  | 48.1        |
| Jelutung      | Light            | 596                                     | 15.3                             | 2.6         | 18.5                 | 0.7             | 3.8         | 0.46 <sup>a</sup>           | 0.1                  | 29.3        |

Note : Keranji,a ; Resak,b ; White Meranti,c ; Kedondong,d ; Jelutung,e

### 3.4 Comparison with EC5 Conductive Model and Density Influence on Charring Rate

Figure 8 presents a comparative evaluation between the experimentally determined charring rates for selected Malaysian tropical hardwoods and the design value stipulated in Eurocode 5 (2004) for hardwoods with densities exceeding 450 kg/m<sup>3</sup>. According to Eurocode 5 (2004), a one-dimensional charring rate of 0.5 mm/min is recommended under standard fire exposure conditions. The experimental data in this study revealed that five of the tested species exhibited charring rates lower than the Eurocode 5 (2004) reference line, indicating superior fire resistance performance relative to the conservative assumption adopted in the standard. This deviation from the Eurocode 5 (2004) threshold demonstrates the potential of certain tropical hardwoods for structural use in fire-sensitive applications, provided that their performance is adequately characterized.

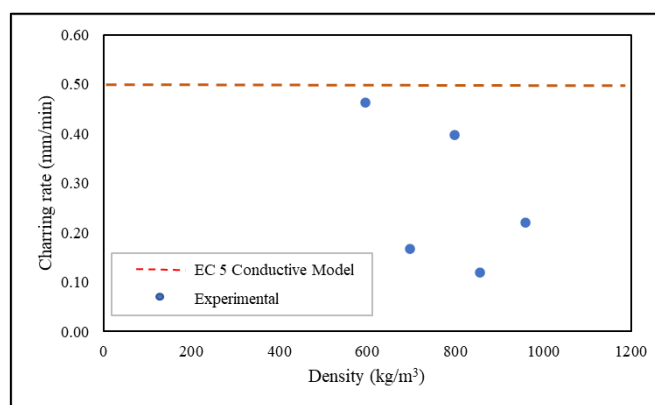
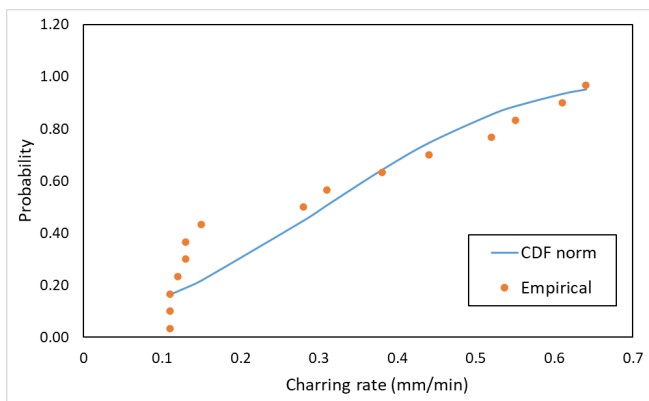


Figure 8. Comparison of experimental results with Eurocode 5 model

### 3.5 Cumulative Distribution of Charring Rate Across Tropical Hardwood Species

Figure 9 displays the cumulative distribution function (CDF) of charring rates for five selected Malaysian tropical hardwood species, compared with the empirical data. The empirical cumulative distribution function (ECDF), represented by orange data points, is plotted alongside a

theoretical normal cumulative distribution function (NCDF) shown as a blue line. This comparison enables the evaluation of how closely the observed data conforms to a Gaussian distribution.



**Figure 9.** Cumulative Distribution Curve of Charring Rate for 5 species

The empirical data closely follows the shape of the NCDF, indicating that the charring rate distribution may reasonably approximate a normal distribution. Some deviations are visible at the lower and upper tails, where empirical probabilities slightly deviate from the theoretical curve. This deviation is likely associated with species-specific effects or variability in material properties (e.g., density, moisture content). At the lower end of the distribution, within the charring rate range of 0.1–0.2 mm/min, the ECDF rises more steeply than the NCDF, indicating a higher frequency of low charring rate values than would be expected under a normal distribution. These values are primarily associated with species such as Keranji (959 kg/m<sup>3</sup>) and White Meranti (856 kg/m<sup>3</sup>), both of which possess higher densities and demonstrated greater resistance to thermal degradation. Studies have shown that lower-density samples often exhibit reduced thermal conductivity, resulting in faster surface temperature rise and earlier pyrolysis, whereas higher density samples lead to slower surface heating and reduced charring rates (Bartlett et al., 2019; Friquin, 2010)

In the mid-range of the distribution (approximately 0.25–0.45 mm/min), the empirical points exhibit good alignment with the NCDF, suggesting that in this interval, the charring rate data reasonably follow a normal distribution. This region represents species such as Kedondong and Jelutong, which are characterized by lower densities (698 kg/m<sup>3</sup> and 596 kg/m<sup>3</sup> respectively) and moderate to high moisture content. These species exhibit more predictable pyrolysis responses, likely influenced by more uniform internal structures and moisture-driven heat absorption.

Toward the upper tail of the distribution (above 0.5 mm/min), the empirical values again deviate from the

theoretical curve, lying below the NCDF. This divergence suggests that fewer samples recorded extremely high charring rates than expected under the normal model. Resak, although categorized as medium density (799 kg/m<sup>3</sup>), contributes to this segment because of its propensity to develop deep surface cracks under high thermal exposure, accelerating char development. Cracking under fire exposure is a known phenomenon that can increase localized surface area, thereby intensifying degradation.

Overall, the NCDF provides a useful reference for understanding the probabilistic trend of charring behavior; however, the discrepancies at the distribution extremes highlight the importance of considering anatomical and physical variability across wood species. While the normal model may serve as a useful approximation in preliminary risk assessments and model development, reliance on empirical distribution is essential for species-specific fire performance evaluations, especially when dealing with naturally variable materials like tropical hardwoods.

#### 4. CONCLUSION

In conclusion, this study provides important experimental insights into the one-dimensional charring behavior of selected Malaysian tropical hardwoods under standard fire exposure. The key findings are summarized as follows:

- All tested hardwood species (Keranji, Resak, White Meranti, Kedondong, and Jelutong) exhibited charring rates significantly below the values assumed in design codes. Measured char rates ranged from ~0.12 to 0.46 mm/min, whereas in Eurocode 5, notional design rate for hardwoods is up to 0.50–0.65 mm/min. This indicates that these tropical timbers possess higher inherent fire resistance than the conservative assumptions typically adopted in current design standard.
- While higher wood density generally contributed to slower charring—as observed for the denser species Keranji and White Meranti—density alone did not fully govern the results. Certain lower-density species exhibited slower charring than some higher-density ones, emphasizing the importance of species-specific anatomical traits, such as grain structure, oxygen permeability, and char layer formation. These findings are consistent with previous studies showing that microstructural factors can exert greater influence on charring behaviour than bulk density alone.
- All specimens had moisture contents between 18 % and 22 %, within which no dominant effect on overall charring rates was observed. Nonetheless, higher moisture levels were found to delay ignition and reduce charring in the

early stages of exposure. Hence, the present results are most applicable to air-dry timber condition; significantly wetter (green) wood would be expected to char even more slowly initially due to the heat spent in evaporating water.

- The substantially slower charring rates of these hardwoods suggest that current design guidelines (developed largely for softwoods) are conservative for tropical hardwood applications. Structural designers using such species can anticipate greater residual cross-sections and load-bearing capacity after a given fire duration than predicted by generic code values. This could be leveraged to optimize structural dimensions or to justify the use of local hardwood species in fire-sensitive applications, provided that adequate safety factors and validation are applied. This finding supports the development of refined charring models or code provisions that explicitly account for species type, especially for dense hardwoods common in the tropics.
- The thermocouple-based instrumentation method used in this research proved effective for quantifying one-dimensional charring. It enabled accurate temperature tracking and char depth determination and can be adopted in future studies for building a more comprehensive database of charring rates. Such data will enhance fire design calculations and facilitate performance-based engineering of timber structures.

Overall, the research demonstrates that Malaysian tropical hardwoods exhibit excellent fire performance due to their slow charring behavior. By quantifying these rates, this study establishes a reliable basis for improved fire design involving tropical timber. Future work should extend this investigations to additional species and larger structural elements (e.g. glulam or cross-laminated timber elements), to validate the findings and promote their integration into engineering practice and fire design standards. The results not only contribute to a deeper scientific understanding of wood charring mechanisms but also support the safer and more efficient use of sustainable hardwood materials in modern construction.

## ACKNOWLEDGEMENT

The authors gratefully acknowledge the Ministry of Higher Education for its support and funding of this research under the Fundamental Research Grant Scheme (FRGS) (Grant No. FRGS/1/2023/TK06/UITM/03/1). Special thanks are extended to the Fire Protection Laboratory at the Forest Research Institute Malaysia (FRIM) and the Research Management Centre at Universiti Teknologi MARA (UiTM) for their invaluable laboratory and administrative support.

## REFERENCES

- Bakri, Z., & Ahmad, Z. (2025). *One-Dimensional Charring Rate for Laminated Veneer Lumber from Malaysian Tropical Timber*. 63–82. [https://doi.org/10.1007/978-981-96-5837-4\\_4](https://doi.org/10.1007/978-981-96-5837-4_4)
- Bartlett, A. I., Hadden, R. M., & Bisby, L. A. (2019). A Review of Factors Affecting the Burning Behaviour of Wood for Application to Tall Timber Construction. In *Fire Technology* (Vol. 55, Issue 1). Springer New York LLC. <https://doi.org/10.1007/s10694-018-0787-y>
- Cachim, P. B., & Franssen, J. M. (2010). Assessment of Eurocode 5 charring rate calculation methods. *Fire Technology*, 46(1), 169–181. <https://doi.org/10.1007/s10694-009-0092-x>
- EN 13381-7. (2019). *EN 13381-7: 2019 Test Methods for Determining the Contribution to the Fire Resistance of Structural Members - Part 7 : Applied Protection to Timber Members*.
- Eurocode 5. (2004). *EN 1995-1-2: Eurocode 5: Design of timber structures - Part 1-2: General - Structural fire design*.
- Frangi, A., & Fontana, M. (2003). Charring rates and temperature profiles of wood sections. *Fire and Materials*, 27(2), 91–102. <https://doi.org/10.1002/fam.819>
- Frangi, A., & König, J. (2011). Effect of increased charring on the narrow side of rectangular timber cross-sections exposed to fire on three or four sides. *Fire and Materials*, 35(8), 593–605. <https://doi.org/10.1002/fam.1078>
- Friqui, K. L. (2010). *Charring rates of heavy timber structures for Fire Safety Design : A study of the charring rates under various fire exposures and the influencing factors*.
- Friqui, K. L. (2011). Material properties and external factors influencing the charring rate of solid wood and glue-laminated timber. *Fire and Materials*, 35(5), 303–327. <https://doi.org/10.1002/fam.1055>
- Hugi, E., Wuersch, M., Risi, W., & Ghazi Wakili, K. (2007). Correlation between charring rate and oxygen permeability for 12 different wood species. *Journal of Wood Science*, 53(1), 71–75. <https://doi.org/10.1007/s10086-006-0816-1>
- ISO 834. (1999). *ISO 834-1 Fire-resistance tests-Elements of building construction-Part 1: General requirements*. [www.sis.se](http://www.sis.se).
- Liu, J., & Fischer, E. C. (2024). Review of the charring rates of different timber species. *Fire and Materials*, 48(1), 3–15. <https://doi.org/10.1002/fam.3173>
- Luptáková, J., Kačík, F., Mitterová, I., & Zachar, M. (2019). Influence of temperature of thermal modification on the fire-technical characteristics of Spruce Wood. *BioResources*, 14(2), 3795–3807. <https://doi.org/10.15376/biores.14.2.3795-3807>
- MacLeod, C. E., Law, A., & Hadden, R. M. (2023). Quantifying the heat release from char oxidation in timber. *FIRE SAFETY JOURNAL*, 138. <https://doi.org/10.1016/j.firesaf.2023.103793>
- Martinka, J., Rantuch, P., & Liner, M. (2018). Calculation of charring rate and char depth of spruce and pine wood from mass loss. *Journal of Thermal Analysis and Calorimetry*, 132(2), 1105–1113. <https://doi.org/10.1007/s10973-018-7039-8>
- Morrisset, D., Hadden, R. M., Bartlett, A. I., Law, A., & Emberley, R. (2021). Time dependent contribution of char oxidation and flame heat feedback on the mass loss rate of timber. *Fire Safety Journal*, 120. <https://doi.org/10.1016/j.firesaf.2020.103058>
- MS 544 : Part 9. (2001). *MS 544 : Part 9 : Section 1 : 2001 Code of Practice for Structural Use of Timber: Part 9 : Fire Resistance of Timber Structures : Section 1 : Method of Calculating Fire Resistance of Timber Members*.
- Njankouo, J. M., Dotreppe, J. C., & Franssen, J. M. (2004). Experimental study of the charring rate of tropical hardwoods. *Fire and Materials*, 28(1), 15–24. <https://doi.org/10.1002/fam.831>
- Osvaldova, L. M., Kosutova, K., Lee, S. H., & Fatriasari, W. (2023). Ignition and burning of selected tree species from tropical and northern temperate zones. *Advanced Industrial and Engineering Polymer Research*, 6(2), 195–202. <https://doi.org/10.1016/j.aiepr.2023.01.006>
- Qin, R., Zhou, A., Chow, C. L., & Lau, D. (2021). Structural performance and charring of loaded wood under fire. *Engineering Structures*, 228. <https://doi.org/10.1016/j.engstruct.2020.111491>
- Richter, F., Atreya, A., Kotsovinos, P., & Rein, G. (2019). The effect of chemical composition on the charring of wood across scales. *Proceedings of the Combustion Institute*, 37(3), 4053–4061. <https://doi.org/10.1016/j.proci.2018.06.080>
- Richter, F., Kotsovinos, P., Rackauskaite, E., & Rein, G. (2021). Thermal Response of Timber Slabs Exposed to Travelling Fires and Traditional Design Fires.

- Fire Technology*, 57(1), 393–414. <https://doi.org/10.1007/s10694-020-01000-1>
- UBBL. (2024). *UNIFORM BUILDING BY LAWS 1984* (International Law Book Services, Ed.). Laws of Malaysia.
- Wang, X., Zhang, S., & Wan, Z. (2025). Charring rate and temperature distribution of timber in fire: The role of fire-retardant treatments, moisture, and tree species. *Structures*, 75. <https://doi.org/10.1016/j.istruc.2025.108676>
- Wen, L., Han, L., & Zhou, H. (2015). Factors Influencing the Charring Rate of Chinese Wood by using the Cone Calorimeter. *BioResources*, 10(4), 7263–7272. <https://doi.org/10.15376/biores.10.4.7263-7272>
- Werther, N., & Matthäus, C. (2020). Factors influencing the charring behaviour of timber. *BAUTECHNIK*, 97(8), 540–548. <https://doi.org/10.1002/bate.201900112>
- Zhang, J., Liu, Z. H., Xu, Y. X., Ma, S. W., & Xu, Q. F. (2012). An experimental and numerical study on the charring rate of timber beams exposed to three-side fire. *Science China Technological Sciences*, 55(12), 3434–3444. <https://doi.org/10.1007/s11431-012-4996-1>